ELSEVIER

Thermochimica Acta 249 (1995) 143–159

thermochimica acta

Direct calorimetry of aquatic animals: dynamic response of biological processes

Vincent J.T. van Ginneken[a,*], Jan Vanderschoot[b], Albert D.F. Addink[a], Guido E.E.J.M. van den Thillart[a]

[a]*Animal Physiology, Department of Biology, University of Leiden, Gorlaeus Labs., Einsteinweg 55, P.O. Box 9502, 2300 RA Leiden, The Netherlands*

[b]*Medical Informatics, Department of Medicine, Wassenaarseweg 62, P.O. Box 9604, 2300 RC Leiden, The Netherlands*

Received 2 February 1994; accepted 21 July 1994

Abstract

The theory of system identification was used to determine the time constant τ of a 1 litre flow through differential calorimeter (Setaram GF 108) at a flow rate of 50 ml min^{-1}. By numerical differentiation the impulse response function $g(t)$, the time derivative of the step response $f(t)$, was calculated. With the aid of the Prony method, the time constant a_2 of the time-discrete system of the decimated dataset was calculated, giving a mean value of 0.7402 ± 0.0044 ($n = 4$). This value was converted to the time constant τ of the time-continuous system, giving a value of 33.25 ± 0.65 min ($n = 4$). The description of the system agreed with a model for a first order process. For control of the time constant value, the step response $f(t)$ and the impulse response $g(t)$ signal were simulated from the original block diagram $u(t)$ which gave a suitable fit. Via the technique of deconvolution, the datasets of a biological case study with goldfish (*Carassius auratus* L.) were desmeared to describe the dynamic responses of the biological processes in the calorimetric vessel with a much reduced time constant τ. Finally, the timescale on which the process of metabolic depression takes place in this species during anaerobiosis was estimated to be several minutes.

Keywords: Biological system; Deconvolution; Fish; Kinetics; Metabolic rate; Time constant

* Corresponding author.

SSDI 0040-6031(94)02033-7

1. Introduction

The metabolic rate, the energy per unit of time ($P = \delta Q/\delta t$), is an important physiological parameter reflecting the intensity of a biological process. It can be characterized by detecting the heat production (direct calorimetry), or it can be derived from the oxygen consumption by means of an oxycaloric value (indirect calorimetry) [1].

Moreover, calorimetry is the only (biophysical) method by which to register the sum of aerobically and anaerobically produced heat which is necessary for quantification of both types of metabolism.

A calorimetric system build by Setaram (Lyon, France) has been further developed in our laboratory to study those parameters for large aquatic animals during long term experiments under stress-free conditions [2]. To be able to perform this kind of experiment, the calorimeter is equipped with a flow through system. Constant experimental conditions can be maintained because fresh water is supplied and metabolic waste products are flushed out. The system was improved by providing an automated data acquisition system, which enables us to collect in a very accurate way the linked datasets of heat production and oxygen consumption of the animals in one of the compartments [3]. In this way we studied the effects of such adverse environmental conditions as hypoxia [4,5] and anoxia [5–8]. Under these conditions the organisms decrease their metabolic rate below the standard rate, which is the maintenance level under normoxia. The reduction of both oxygen consumption and heat production, called metabolic depression [3–8] can be acquired only by the technique of calorimetry. The recorded signal corresponds to the detected power in the biological process. Little information can be acquired about the kinetics of the biological process because of the long response time of the system (the lag time). To clarify the role of the calorimeter and correct for the deformation of the signal because of lag, the principles of heat flow and heat detection in the calorimeter need to be understood.

1.1. Principle of heat flow

The heat flow in a calorimeter can be divided into two components: the heat exchange between the sample and the calorimeter (heat transfer coefficient) and the heat content of the sample (heat capacity). The heat flow can be expressed in the time constant τ of the system [9]

$$\tau = C_p/G \tag{0}$$

in which C_p is the heat capacity and G is the thermal conductance.

Obviously, for our flow through calorimeter, a constant flow through the cell does not influence τ, it only lowers the efficiency of measurement, as a constant part of the generated heat will "leak out". The efficiency as a function of the flow rate has been described: for a flow of 50 ml min^{-1} it was found to be 87% (see fig. 3 of Ref. [2]).

One of the aims of this paper is to describe the time constant τ of the Setaram GF 108 calorimeter at a flow rate of 50 ml min^{-1}.

1.2. Principle of heat detection

Thermopiles surround the experimental vessel and detect the temperature difference between the vessel and the thermostatted calorimetric metal block that functions as a heat sink. The temperature difference is a reflection of the thermal power in the vessel [10]. The voltage signal of the thermopiles is proportional to the temperature difference between the vessel and the heat sink. To eliminate any bias caused by thermal instability of the calorimetric block, differential detection is applied.

Most of the generated heat is detected by the thermopiles. The sensitivity coefficient derived in the calibration procedure corrects the signal for two types of heat losses: (a) heat losses in general to the surroundings, and (b) minor heat losses caused by the outflowing water (see fig. 3 of Ref. [2]).

By integration, the area under the curve of the detected signal is calculated. If the rate of the process in the vessel is constant the thermal power corresponds to the detected signal. When the signal is delayed owing to the time constant of the system, the detected signal is smoothed. This effect is known as smearing [11]. When the time constant of the system is known, the detected signal can be mathematically manipulated afterwards (desmeared) to find the "real" response of the biological system in the vessel. The most comprehensive paper on this subject of dynamic corrections for calorimeters is that of Randzio and Suurkuusk [10]. More recently, with the increasing application of the computer as a laboratory tool, the technique of model simulation based on computer techniques has attracted more interest. In this paper we used the theory of system identification given by Ljung [12] to describe the dynamic properties of our calorimetric system on an MS-DOS 386 personal computer.

The aim of this paper is to describe the time constant τ of a Setaram GF 108 flow through differential calorimeter at a flow rate of 50 ml min^{-1} and to apply this to the data from a biological case study with goldfish (*Carassius auratus* L.) in order to eliminate the effect of the heat capacity on the detected heat flow.

From the deconvoluted signal we determined the timescale on which the process of metabolic depression takes place in this species when exposed to anoxia.

2. Materials and methods

The theory of convolution, deconvolution and impulse response is described elsewhere [12,13] but some background theory will be given in Section 2.1. In Section 2.2 the applied procedure will be described. Section 2.3 will describe the experimental setup for a biological case study with goldfish.

2.1. Background theory

A time-continuous system, like a calorimeter, for which we may assume that the behaviour is linear and time invariant, can be described by the following

mathematical model

$$y(t) = \int_{-\infty}^{t} g(t-\tau)u(\tau)\mathrm{d}\tau \tag{1}$$

in which $y(t)$ is the response of the system, $u(t)$ is the input to the system and $g(t)$ is the impulse response of the system. The right-hand side of Eq. (1) is known as the convolution of the function u with the function g. Note that the system is completely described by g. Deconvolution is the inverse operation, i.e., it maps the pair (y, g) into u. In practice, deconvolution can be described as a convolution with a function derived from g, the impulse response of the *inverse filter*.

The determination of g, given a set of simultaneous signals y and u, is the subject of systems identification. If the necessary calculations are carried out by means of a digital computer, both signals have to be sampled. If the sampling interval is T, the result is a set of time-discrete signals $\tilde{y}$ and $\tilde{u}$. They are related to the original signals by

$$\tilde{u}(k) = u(kT), \quad \tilde{y}(k) = y(kT) \tag{2}$$

If the sampling rate satisfies the Nyquist criterion, and if we may assume that the time-continuous input $u(t)$ is constant between the sampling instants, then the sampled signals are related by

$$\tilde{y}(k) = \sum_{i=-\infty}^{k} \tilde{g}(k-i)\tilde{u}(i) \tag{3}$$

in which $\tilde{g}(k)$ is the impulse response of some time-discrete system. System identification techniques aim at the determination of $\tilde{g}(k)$. Note that, if $\tilde{g}(k)$ is known, then the sampled response of the original system can be calculated for every input $u(k)$ satisfying the above conditions. It is clear that g and $\tilde{g}$ must be related to one another. This relationship can be derived for a large class of time-continuous systems. However, we are only interested in a simple first-order system here

$$\dot{y} = ay + bu \tag{4}$$

which has an impulse response

$$g(t) = b\mathrm{e}^{at} \quad \text{for} \quad t \geqslant 0 \tag{5}$$

$$= 0 \qquad \text{for} \quad t < 0 \tag{6}$$

Note that Eq. (4) is identical to the so called Tian–Calvet equation after some appropriate substitutions. However, we prefer the notation of Eq. (4) as being a standard form of the state space description of dynamic systems. Such a standard form facilitates the application of known techniques for system identification, and avoids the invention of yet another naive technique.

The constant $-1/a$ is known as the time constant. On the other hand, the impulse response of a first-order time-discrete system

$$\tilde{y}(k+1) = \tilde{a}\tilde{y}(k) + \tilde{b}\tilde{u}(k) \tag{7}$$

is given by

$$\tilde{g}(k) = \tilde{b}\tilde{a}^k \quad \text{for} \quad k \geqslant 0 \tag{8}$$

$$= 0 \quad \text{for} \quad k < 0 \tag{9}$$

If the discrete time system must be equivalent to the time-continuous system, then we must have

$$\forall k: \quad g(kT) = \tilde{g}(k) \tag{10}$$

in which T is the sampling interval. Therefore, it must be that

$$\forall k: \quad b\mathrm{e}^{akT} = \tilde{b}\tilde{a}^k \tag{11}$$

This is true if and only if

$$b = \tilde{b} \tag{12a}$$

and

$$\mathrm{e}^{aT} = \tilde{a} \tag{12b}$$

Having determined $\tilde{b}$ and $\tilde{a}$ for a given set of samples $\tilde{y}(k)$ and $\tilde{u}(k)$, by means of a system identification technique, it is then possible to estimate the time constant of the original system by $-1/a = -T/\ln\tilde{a}$. The identification method applied in this research project is the Prony method. This method determines coefficients a_1, a_2, ... and b_1, b_2, ... such that the impulse response of the model

$$\sum_{i=1}^{n_a+1} a_i\tilde{y}(k-i+1) = \sum_{i=1}^{n_b+1} b_i\tilde{u}(k-i+1) \tag{13}$$

fits a given sequence $\tilde{g}(k)$. The numbers n_a and n_b must be specified beforehand, and b_1 is always chosen by the method such that $a_1 = 1$. If $n_a = 1$ and $n_b = 0$, we obtain the model

$$\tilde{y}(k+1) + a_2\tilde{y}(k) = b_1\tilde{u}(k) \tag{14}$$

This is the same model as in Eq. (7) with $\tilde{a} = -a_2$. Therefore the time constant of the original time-continuous system can now be estimated from

$$\tau = -1/a = -T/\ln(\tilde{a}) = -T/\ln(-a_2) \tag{15}$$

For practical reasons it is not possible to record an impulse response from the calorimeter, therefore a step response has been utilized. This constitutes no special problem, because the impulse response is the time derivative of the step response and can, therefore, be estimated by numerical differentiation.

2.2. *Applied procedure*

The following procedure was applied.

(a) Input and output data were created. The characteristics of the system were determined based on the input data $u(t)$ and the measured output data $y(t)$, the so called system identification [12].

Consequently the data $y(t)$ were decimated, and by numerical differentiation the impulse response function $g(t)$, the time derivative of the step response $f(t)$, was calculated.

(b) A model, the Prony method, was selected and applied to the impulse response $g(t)$. This achieves parameterizing of the time-discrete system, resulting in the time constant a_2.

(c) From this parameter a_2 the time constant τ of the continuous system is calculated following Eq. (15). The derived value for the time constant was checked for validity by simulating the step response $f(t)$ and the impulse response $g(t)$ of the signal.

(d) The simulated signal and the measured output signal were compared for the step response $f(t)$ and the impulse response $g(t)$ signal to check whether the time constant would fit.

(e) With the aid of the time constant τ the recorded data of a case study with goldfish were desmeared.

All mathematical calculations (time constant, simulation step and impulse response) were performed with the software MATLAB. Desmearing of the recorded datasets was carried out using QUATTRO PRO.

2.2.1. Creating input and output data

The method used to obtain the data is based on the calibration procedure described elsewhere [3]. Calibration is performed with a known electrical current and voltage (Setaram EJ2 joule calibrator). To obtain a specific dataset, a current of 3.15 mA with a voltage of 3.164 V is applied to a resistor of 1000 Ω mounted in the measurement vessel, resulting in a power output signal of 9.97 mW. First a baseline was recorded during 20 min, then the impulse was administered during 360 min followed by a return time of 240 min.

A sampling rate of once per minute resulted in a dataset of 717 data points. Because of the limited memory capacity of MATLAB a decimation procedure was applied to the dataset. First, five data points of the dataset were eliminated to avoid the problem of the decimation procedure affecting the registered onset of the signal (712 data points). Subsequently the dataset was detrended and decimated (71 data points). The original block diagram and the time delayed response are depicted in Fig. 1. By numerical differentiation the first derivative $g(t)$ was calculated (Fig. 2). The first negative peak (A) was selected on which to apply the Prony method.

2.2.2. Selection of the model

The computer model used in the simulation technique is considered as a black box. This means that the model parameters have no physical meaning but are simply used to adjust the input data in such a way that they fit to the output data [12].

In the literature several models are described which would be suitable to use [12]. We selected the Prony method as a means of parametric modelling because of its simplicity. This is a technique that is a good alternative to Fourier transformation [14], which is often applied in spectrum analysis of discrete time series [15]. It

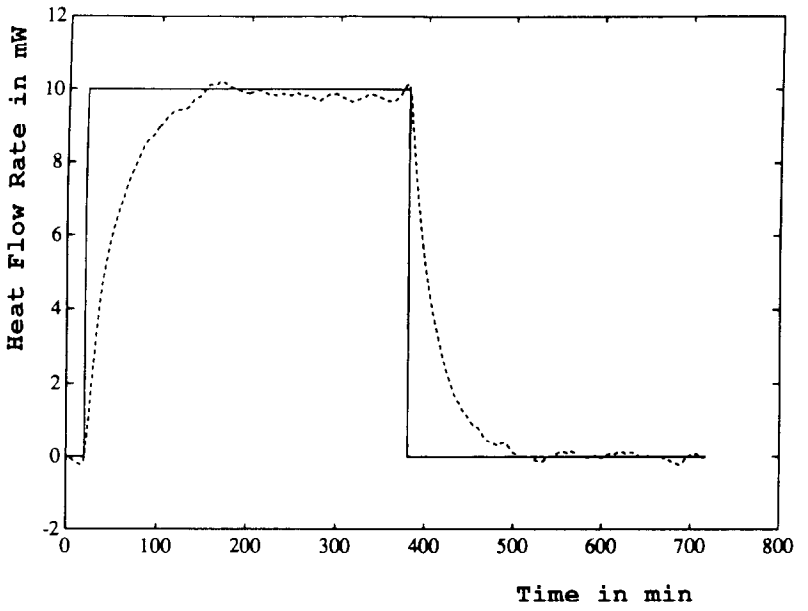

Fig. 1. Calibration procedure by electrical current. An electrical current of 3.15 mA and a voltage of 3.164 V were applied to a resistor of 1000 Ω, resulting in a heat production of 10 mW. The solid line (block diagram) is the input signal $u(t)$. After a waiting time of 20 min the heat pulse is generated by electrical current during a time period of 360 min. The dotted line is the output response (step response $f(t)$) of the calorimeter.

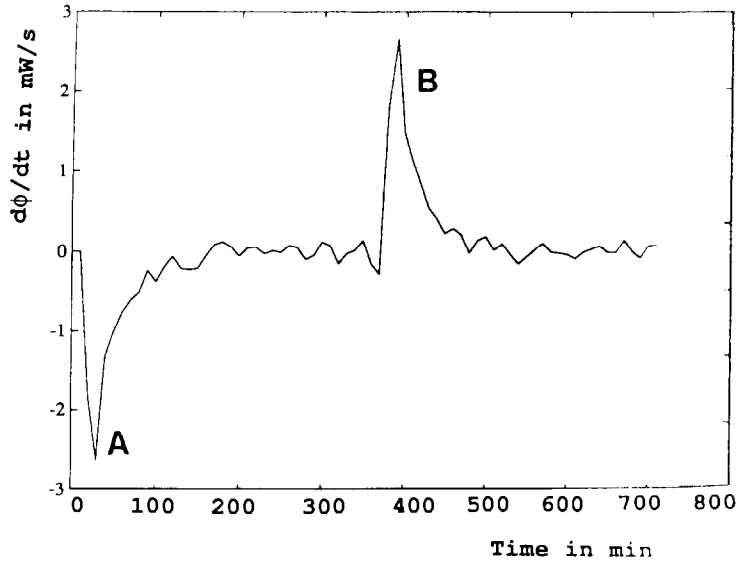

Fig. 2. First derivative of the step response $f(t)$, the impulse response function $g(t)$.

applies a least squares solution to linear equations arising from the convolution matrix formed from the impulse response sequence [16].

2.2.3. Conversion of the time-discrete time constant a_2 into the time-continuous time constant τ

The conversion is described by Eq. (15).

2.2.4. Check the validity of the model

The validity of the model was checked by comparing (a) the fit of the converted input block diagram with the recorded output signal (see Fig. 3); (b) the fit of the recorded impulse response with the simulated signal (see Fig. 4). (c) The area under the curve (AUC) of the original and the manipulated data may not be affected by the mathematical desmearing method. This can be checked by the ratio AUC (original data)/AUC (desmeared data), which should approximate to unity.

2.2.5 Desmearing of the recorded data

Data were desmeared using the time constant τ. Because the signal to noise ratio was increased because of the deconvolution, data were filtered in the spreadsheet. For every new smoothed point the mean value of ten data points was used. Subsequently, for the next smoothed point, the corresponding block of 10 points was moved one place and the average value was calculated. This calculation resulted in the introduction of an artificial time constant of 10 min.

2.3. Experimental setup case study

To derive rough data, the following experiment was performed. Goldfish (*Carassius auratus* L.) were obtained from a commercial fish dealer. They were kept at 20°C under a light regime of 10 h dark and 14 h light at normoxic oxygen levels of 80% air saturation. The animals were fed with Trouvit pelleted food (Putten, The Netherlands).

A group was created of four individuals with a biomass of 6.1, 10.2, 7.5 and 6.5 g respectively. At a flow rate of 50 ml min^{-1} the amount of selected biomass corresponded to an oxygen depletion of $\approx 20\%$ at normoxia. Seven days prior to the experiment the fish were starved under dark conditions outside the calorimeter in an identical calorimetric vessel at a flow rate of 50 ml min^{-1}. This was done for standardization and to eliminate any circadian rhythm. Calibration of the heat signal and detection of oxygen were performed as described elsewhere [3]. Rates of oxygen consumption were calculated according to the Fick principle [17] following

$$\dot{V}_{O_2} = v(c_r - c_m) \quad \text{mg} \quad O_2 \quad h^{-1} \tag{16}$$

where v is the water flow through the vessels; for both vessels $v = 50$ ml min^{-1}. c_r and c_m are respectively the oxygen concentrations measured in the outflowing water of the calorimeter of the reference and the measurement vessel respectively. From a Winkler titration, the value c_r corresponded to 8.84 ± 0.062 mg l^{-1} ($n = 6$).

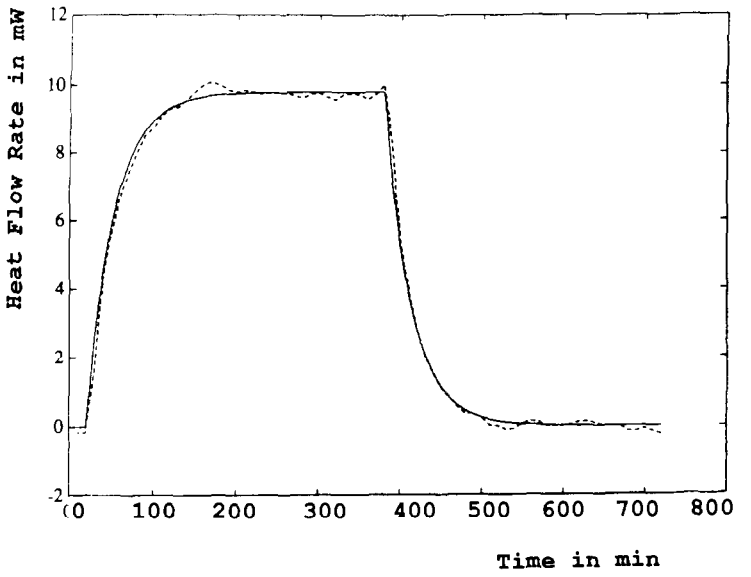

Fig. 3. The dotted line is the output function of the calorimeter (see Fig. 1). The solid line is the simulated signal of the input signal $u(t)$ (block diagram, Fig. 1) based on the time constant a_2 of the time-discrete system of 0.7402 ± 0.0044. The simulated signal gives a nearly exact fit.

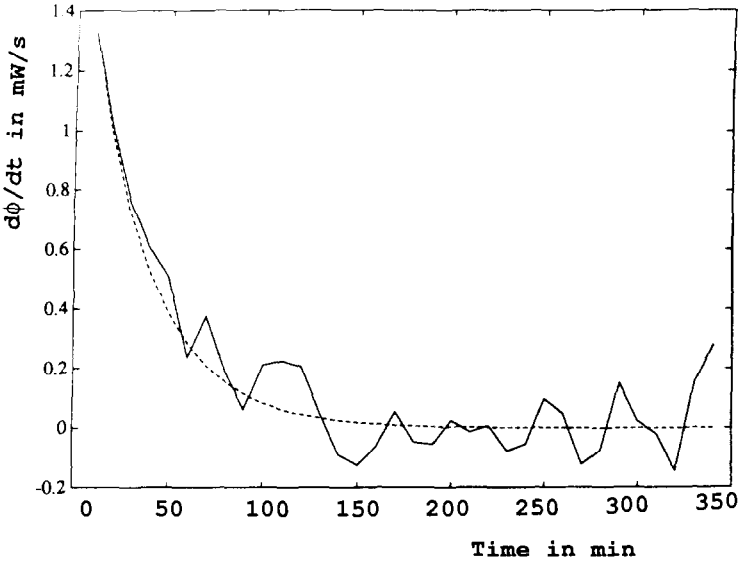

Fig. 4. The irregular solid line is the first slope (A) of the impulse response $g(t)$ (see Fig. 2). The dotted line is the simulated signal of the input signal $u(t)$ (block diagram, Fig. 1) based on the time constant a_2 of the time-discrete system of 0.7402 ± 0.0044.

The case study with goldfish lasted 3 days (sampling rate 1 min, resulting in 4320 data points amplification range 2.5 mV, sampling intervals in the reference and the measuring vessel were 10 min and 70 min respectively) [3]. Anoxia was introduced at the end of the second day by saturating the inlet water with pure nitrogen gas.

3. Results

The 10 mW joule effect procedure resulted in a mean sensitivity coefficient of 87.89 ± 0.55 μV mW^{-1} ($n = 4$). With these values the output functions were created, as depicted in Fig. 3.

By differentiation the impulse response $g(t)$ was calculated (see Fig. 2).

The time constant a_2 of the time-discrete system was 0.7402 ± 0.0043. This means that the signal per unit time has been reduced by 74%. Inserting this value into Eq. (15) and multiplying by the factor 10, because the data were decimated, gives the time constant τ of the time-continuous system as 33.25 ± 0.65 min.

The validity of the model was checked by converting the original block diagram (Fig. 1) with the aid of the calculated time constant of the time-discrete system a_2, and the figures were compared. This gave an almost identical fit (Fig. 3). In Fig. 4 the converted signal of the impulse response is compared with the original recorded signal (the slope of peak A in Fig. 2). This gave an acceptable fit.

The case study with goldfish is depicted in Fig. 5(a). The upper fluctuating signal is the oxygen tension signal of the measurement and reference vessels due to the action of the computer driven valve [3]. The lower signal is the heat flow signal. The experiment is started and finished with an electrical calibration. After approximately 12 h the goldfish ($n = 4$) are introduced into the measurement vessel. The specific heat production over the initial normoxic period (12–39 h) is 2709 mJ h^{-1} g^{-1}. The corresponding oxygen consumption is 6.48 μmol h^{-1} g^{-1} and the oxycaloric coefficient is 422 ± 50.3 kJ mol^{-1}.

At approximately $t = 39$ h, anoxia is introduced, and reoxygenation is introduced at $t = 48$ h. The specific heat production during anoxia is 660 mJ h^{-1} g^{-1}. This corresponds to a reduction of the heat production to 24.4% of the normoxic heat production (interval 12–39 h).

After reoxygenation, the heat production and corresponding oxygen consumption are initially elevated. The specific heat production during reoxygenation (interval 48–56 h) is 3439 mJ h^{-1} g^{-1}, which corresponds to a value of 127% compared with the initial normoxic heat production (interval 12–39 h). The oxygen consumption during the reoxygenation interval is 7.46 μmol h^{-1} g^{-1}.

In Fig. 6 the period of metabolic depression is depicted in enlarged format (selection interval 32–56 h). It can be concluded that the process of metabolic depression in these fish takes place on a timescale of minutes. In the deconvoluted signal during the initial normoxic and anoxic periods some fluctuations in the heat production signal can be noticed, which disappear during reoxygenation.

The third check for correction of the model comprises a comparison of the area under the curves (AUC) of the original dataset (Fig. 5(a)) and the time corrected

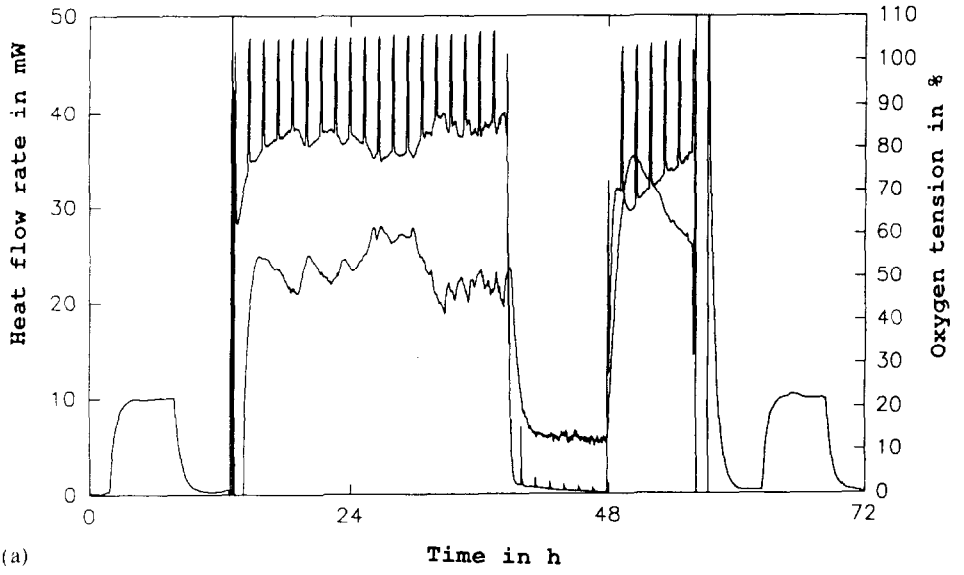

(a)

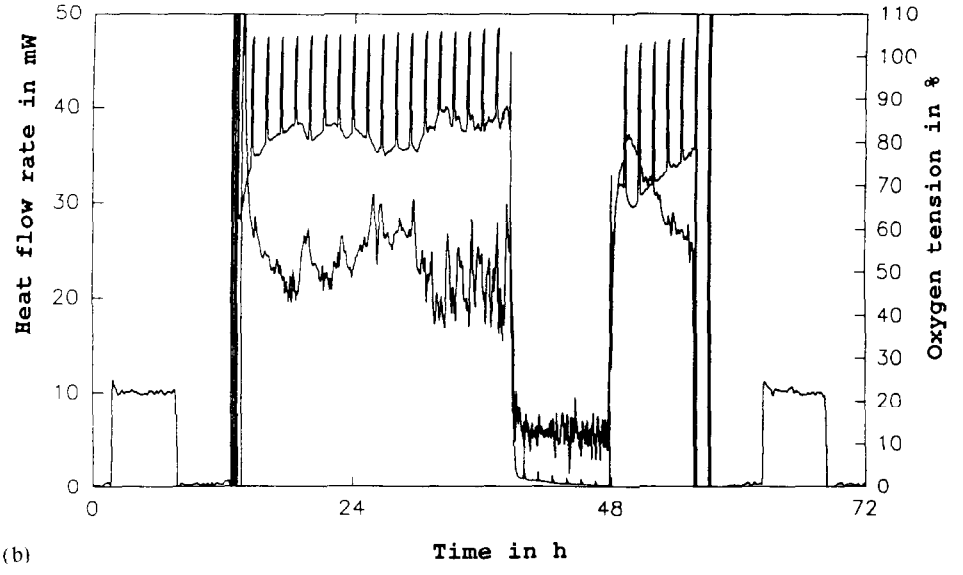

(b)

Fig. 5. (a) Case study with goldfish ($n = 4$) during 3 days. The upper fluctuating signal is the oxygen tension signal (%) measured in the outflow water of the reference or measurement vessel. An alternating rotating valve is directing the outflow along an oxygen electrode. The bottom line is the heat production (mW) of the calorimeter. The experiment is started and finished with an electrical calibration procedure, resulting in a heat production of approximately 10 mW. At the end of the second day anoxia is introduced. The animals respond with metabolic depression, a reduction of the heat production. After reoxygenation there is increased heat production and oxygen consumption. (b) Desmeared signal of the heat flow rate of the experiment as depicted in Fig. 5(a).

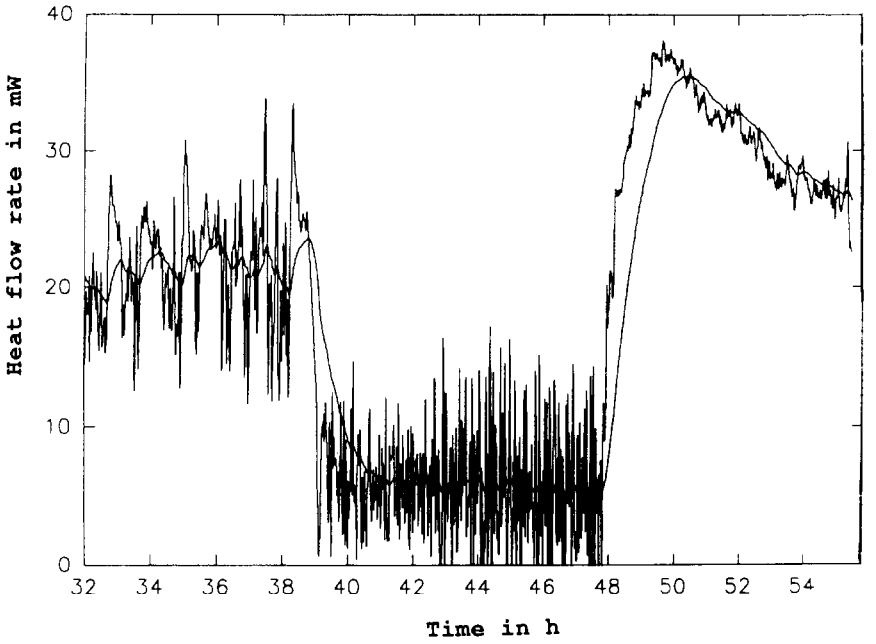

Fig. 6. Enlargement of the registration of the process of metabolic depression as depicted in Fig. 5(a) (recorded signal) and Fig. 5(b) (deconvoluted signal).

dataset (Fig. 5(b)) of the case study performed with goldfish. The AUC of the original and the time corrected dataset was 3 143 620 mJ per 41.78 h and 3 177 601 mJ per 41.78 h respectively ($n = 1$). From these data it can be concluded that the time-corrected dataset is overcorrected by as little as 1.1 %.

4. Discussion

We have described the characteristics of the system by a first order model with one time constant. Concerning the first peak of the signal of the impulse response (Fig. 2, peak A) it can be concluded from the tailing of the first vertical signal that there is a tendency towards a higher order model. However, the first order model we used was suitable because the step and the impulse response gave a perfectly good simulation using the time constant a_2 of the time-discrete system (Figs. 3 and 4).

Because we have found a first order model for the perfusion vessel filled solely with water (no animals), it can be concluded that there is an ideal pattern of mixing in the vessel. If there are animals in the vessel, higher order effects may result due from locomotion and ventilation of the fish [18].

It may be concluded that the time constant τ of the time-continuous system is determined mainly by the heat capacity of the water and the heat transfer coefficient

from water to stainless steel. Also, the time constant τ can be calculated from Eq. (0) in the introduction

$$\tau = C_p/G$$

where the heat capacity C_p of 1 litre of water is 4.2 kJ K^{-1}. The thermal conductance G is described by

$$G = \alpha A \tag{17}$$

where α is the transfer coefficient from water to stainless steel ($\alpha = 50$ W K^{-1} m^{-2}) and A is the exchanging surface of the vessel.

The exchanging surface of the vessel can be described by

$$A = (2\pi rh) + \pi r^2 \tag{18}$$

where $r = 5.4$ cm and $h = 10.8$ cm. Thus A corresponds to $(2\pi \times 5.4 \times 10.8) + \pi \times 5.4^2 = 0.0458$ m^2. Consequently, the thermal conductance is $G = 2.29$ W K^{-1}. Following Eq. (0), the time constant is (4200 J K^{-1})/(2.29 W K^{-1}) = 1834 s, which is 30.6 min. This value agrees with the specifications of Setaram for this 1 l stainless steel perfusion vessel.

The value of the time constant may be improved by reducing the heat transfer coeffficient, for example by a gold or copper coating at the surface of the vessel. However, copper ions are poisonous to fish.

To avoid noise, we filtered the data depicting the mean value of 10 data points, so that we reduced the time constant of the system from ≈ 30 min to a period of 10 min.

In the literature some other time constants for calorimeter chambers are given. For 0.5 and 3.5 cm^3 animal chambers the value was 120–150 s, and for a thin walled glass chamber of volume 150 cm^3 the time constant was 600 s [18]. In a 3.5 ml stainless steel perfusion chamber $t_1 = 420$ s and $t_2 = 14\,000$ s [19]. In other work with a 3.5 ml stainless steel perfusion chamber, a value of 151 s for the first order time constant was reported [20]. From these values it can be concluded that the time constant τ for small chambers used in microcalorimetry is < 7 min. In our case, for the 1 l perfusion chamber, the time constant was > 30 min. With increasing size of chamber the time constant τ increases. This can be explained by an increased heat capacity due to a larger volume of water in the chamber and a decreased heat conduction, which can be ascribed to a decreased surface to volume ratio and longer thermal diffusion pathways [18]. From these data it is evident that the technique of deconvolution is of special interest for calorimetric systems with large volume chambers to correct for the time constant of the system.

For creation of the output signal we used the separate signals of each joule effect procedure and not the mean of several runs, because this would affect the point of onset of the input signal. Further, because the decimation procedure also could affect the point of onset of the recorded signal, we eliminated the first five data points of the stable initial plateau (waiting time 20 min, sampling rate 1 per min).

For the oxygen tension signal, likewise, an estimation of the time constant of the system can be made. This time constant approximates the volume of the vessel divided by the flow rate: 1000 ml/(50 ml min^{-1}) = 20 min.

In a previous study, the process of metabolic depression was demonstrated for goldfish during anoxia by using direct calorimetry [5–8]. Values of the metabolic rate during anaerobiosis decreased to levels of $\approx 30\%$ of the normoxic value, which corresponds to the level of metabolic depression of goldfish detected in this study, 24.4% of the normoxic value. This value for a depressed metabolic rate is supported by indirect calorimetric work with anoxic goldfish, estimating an anoxic metabolic rate of 20–30% of normoxic rate [21]. It was further calculated for goldfish in a biochemical study, based on the sum of accumulated end products and depletion of endogenous ATP, phosphagen and O_2 reserves, that the metabolic rate was depressed to one third of normal rates [22].

In this study we estimated for goldfish undergoing anoxia the onset of the process of metabolic depression on a timescale of minutes.

Deconvoluted data (results not shown) of an experiment with *Tilapia* exposed to severe hypoxia showed a metabolic depression on a timescale of 30 min. These data are supported by ^{31}P NMR studies with anoxic goldfish. In the white muscle, a stabilization was noticed of the depletion of creatine phosphate after approximately 30 min of anoxia. It was concluded that this was caused by the energy saving strategy of metabolic depression [23].

In a calorimetric study with common frogs (*Rana temporaria*) [24] the animals were exposed to anoxia by nitrogen gas. Subsequently the metabolic rate decreased to $\approx 30\%$ of the normoxic value in < 20 min and to $\approx 10\%$ of the resting metabolic rate after 40 min. Those data were not corrected for the time constant of the calorimetric system. In a calorimetric study with diving turtle (*Pseudemys scripta elegans*) using a 1.2 l chamber, the metabolic rate declined to 15% of aerobic values within 1 h of anoxia [25]. Again no deconvolution techniques were applied to desmear the detected calorimetric signal.

In contrast, for *Artemia*, using a 3.5 ml chamber, a much faster transition in the hypometabolic state was observed [20]. Via the technique of deconvolution it was demonstrated that 90% of the metabolic depression occurred within 5 min after the onset of aerobic acidosis.

More information on the timescale of the process of metabolic depression can be inferred from the figures in several papers. In a microcalorimeter with a 0.5 ml Pyrex chamber, the oligochaete *Lumbriculus variegatus* exposed to anoxia underwent depression of the metabolic rate from 0.8 to 0.24 mW g^{-1} (30% of the normoxic rate) on a timescale of 50 min [26]. In another study the same species exposed to anoxia reduced the metabolic rate from 63 μW to 20 μW (32% of the normoxic rate) in 2 h, followed by a slight reduction from 20 μW to 17.5 μW in a time of 4 h [27]. The land snail *Oreohelix* spp. during aestivation in a 3.5 ml chamber reduced the metabolic rate from 9 to 4 mW g^{-1} (44% of the control metabolic rate) in 15 min [19]. In a calorimetric study with frogs *Rana temporaria* exposed to anoxia, using a 100 ml chamber, the heat production decreased from

5 mW to 1 mW (20% of the normoxic rate) in ≈ 50 min [28]. It may be observed from these calorimetric studies that there is a large variance in the timescale of the process of metabolic depression, varying from 15 min to 2 h. The time constant for these microcalorimetric chambers may be several minutes, so correction via deconvolution techniques probably does not affect the acquired time periods to any great extent. The data in this study indicate that the process of metabolic depression takes place on a timescale of several minutes. Because we reduced the time constant to 10 min we can not give an exact value, but probably the decrease of the metabolic rate is a directly correlated response to the decrease of the oxygen tension.

The rapid fluctuations of the deconvoluted heat signal during the initial normoxic period and during anoxia (Figs. 5b and 6) are difficult to explain. Because this phenomenon is not observed during the electrical calibration procedure, one may conclude that it is not caused by instrumental bias but must originate from the animals. Furthermore, during reoxygenation the fluctuations have disappeared. To elucidate this problem we intend to record mobility with a video tracking system.

Metabolic depression may be a common strategy among hypoxia tolerant fish species; the underlying mechanism, however, is unknown. In his review Ultsch [29] mentions some mechanisms postulated by other authors, such as changes in concentrations and activities of key glycolytic enzymes, changes in ion flux rates through membranes, and the production of a "stress protein" in response to lack of oxygen. For hibernating mammals it has been suggested that opioids may contribute to a lowering of the metabolic rate, thus conserving energy and water [30,31]. This view was supported by the observation that hibernating hamsters arouse after injection with the opioid antagonist naloxone [30].

For fish, however, further studies need to be performed to elucidate the mechanism of metabolic depression.

5. Conclusions

We have calculated the time constant τ of the Setaram GF108 flow through differential calorimeter at a flow rate of 50 ml min^{-1}. Via a deconvolution technique, we could estimate the kinetic response of biological processes in the vessel. It was concluded for goldfish exposed to anoxia that the process of metabolic depression takes place on a timescale of minutes.

Acknowledgements

V. van Ginneken is supported by a grant from the Foundation for Fundamental Biological Research (BION), which is subsidized by the Netherlands Organization for Scientific Research (NWO), Bion-project no. 427024.

References

[1] K. Blaxter, The Energy Metabolism of Animals and Man, Cambridge University Press, 1989, 336 pp.

[2] A.D.F. Addink, G. van den Thillart, H. Smit and J. van Waversveld, A novel 1 litre flow-through calorimeter for heat production measurements on aquatic animals without stress, Thermochim. Acta, 193 (1991) 41–48.

[3] V.J.T. van Ginneken, A. Gluvers, R.W. van der Linden, A.D.F. Addink and G.E.E.J.M. van den Thillart, Direct calorimetry of aquatic animals: automated and computerized data-acquisition system for simultaneously direct and indirect calorimetry in aquatic animals, Thermochim. Acta, 247 (1994) 209–224.

[4] I. Hardewig, A.D.F. Addink, M.K. Grieshaber, H.O. Pörtner and G. van den Thillart, Metabolic rates at different oxygen levels determined by direct and indirect calorimetry in the oxyconformer *Sipunculus nudus*, J. Exp. Biol., 157 (1991) 143–160.

[5] J. van Waversveld, A.D.F. Addink and G. van den Thillart, The anaerobic energy metabolism of goldfish measured by simultaneous direct and indirect calorimetry during anoxia and hypoxia, J. Comp. Physiol., 159 (1989) 263–268.

[6] J. van Waversveld, A.D.F. Addink, G. van den Thillart and H. Smit, Direct calorimetry on free swimming goldfish at different oxygen levels, J. Therm. Anal., 33 (1988) 1019–1026.

[7] J. van Waversveld, A.D.F. Addink and G. van den Thillart, Simultaneous direct and indirect calorimetry on normoxic and anoxic goldfish, J. Exp. Biol., 143 (1989) 325–335.

[8] J. van Waversveld, The energy metabolism of goldfish at different oxygen levels determined by simultaneous direct and indirect calorimetry, Ph.D. Thesis, State University of Leiden, 1988.

[9] P.C. Gravelle, Heat-flow microcalorimetry and its application to heterogeneous catalysis, Adv. Catal., 24 (1975) 191–263.

[10] S.L. Randzio and J. Suurkuusk, Interpretation of calorimetric thermograms and their dynamic corrections, in A.E. Beezer (Ed.), Biological Microcalorimetry, Academic Press, London, 1980, pp. 311–341.

[11] K.H. Schönborn, On the time lag between thermal event and measuring signal in a heat flux calorimeter, Thermochim. Acta, 69 (1983) 103–114.

[12] L. Ljung, System Identification: Theory for the User, Prentice-Hall International, London, 1987, 234 pp.

[13] A. Belaud, Y. Trotter and C. Peyraud, Continuous evaluation of P_{a,O_2} in fish: recording and data processing, J. Exp. Biol., 82 (1979) 321–330.

[14] S.M. Kay, Modern Spectrum Estimation, Theory and Application, Signal Processing Series, A. v. Oppenheim (Ed.), Prentice-Hall, 1988, 543 pp.

[15] T. Yamane, S. Katayama and M. Todoki, Application of deconvolution method to kinetic studies with conduction type calorimeters, Thermochim. Acta, 183 (1991) 329–338.

[16] T.W. Parks and C.S. Burrus, Digital Filter Design, John Wiley and Sons, 1987, 226pp.

[17] A. Fick, Über die Messung des Blutquantums in den Herzventrikeln, Sitzungsber. Phys. Med. Ges. Würzburg, 16 (1870).

[18] E. Gnaiger, J.M. Shick and J.Widdows, Metabolic microcalorimetry and respirometry of aquatic animals, in C.R. Bridges and P.J. Butler (Eds.), Techniques in Comparative Respiratory Physiology, An Experimental Approach, Society for Experimental Biology Seminar Series, Cambridge University Press, 1989.

[19] B.B. Rees and S.C. Hand, Heat dissipation, gas exchange and acid–base status in the land snail *Oreohelix* during short-term estivation, J. Exp. Biol., 152 (1990) 77–92.

[20] S.C. Hand and E. Gnaiger, Anaerobic dormancy quantified in *Artemia* embryos: a calorimetric test of the control mechanism, Science, 239 (1988) 1425–1427.

[21] J. Andersen, Anaerobic resistance of *Carassius auratus* (L.), Ph.D. Thesis, Australian National University, Canberra, 1975.

[22] G. van den Thillart, F. Kesbeke and A. van Waarde, Influence of anoxia on the energy metabolism of the goldfish, *Carassius auratus* L. Comp. Biochem. Physiol., 59A (1976) 329–336.

[23] G. van den Thillart, A. van Waarde, H.J. Muller, C. Erkelens, A.D.F. Addink and J. Lugtenburg, Fish muscle energy metabolism measured by *in vivo* ^{31}P-NMR during anoxia and recovery, Am. J. Physiol., 256 (1989) R922–R929.
[24] G. Wegener, R. Michel and M. Thuy, Anoxia in lower vertebrates and insects: Effects on brain and other organs, Zool. Beitr. N.F., 30 (1986) 103–124.
[25] D.C. Jackson, Metabolic depression and oxygen depletion in the diving turtle, J. Appl. Physiol., 24 (1968) 503–509.
[26] E. Gnaiger, Direct calorimetry in ecological energetics. Long term monitoring of aquatic animals, Experientia (Suppl.), 37 (1979) 155–165.
[27] E. Gnaiger and I. Staudigl, Aerobic metabolism and physiological responses of aquatic oligochaetes to environmental anoxia: heat dissipation, oxygen consumption, feeding and defecation, Physiol. Zool., 60 (1987) 659–677.
[28] C. Schultz, M. Thuy and G. Wegener, Heat production under normoxic and hypoxic conditions: a microcalorimetric study using a gas flow system, Thermochim. Acta, 187 (1991) 71–78.
[29] G.R. Ultsch, Ecology and physiology of hibernation and overwintering among freshwater fishes, turtles, and snakes, Biol. Rev., 64 (1989) 435–516.
[30] D.L. Margulus, Beta-endorphin and endoloxone: Hormones of the autonomic nervous system for the conservation or expenditure of bodily resources and energy in anticipation of famine or feast, Neurosci. Biobehav. Rev., 3 (1979) 155–162.
[31] P.W. Hochachka and M. Guppy, Estivators, in Metabolic Arrest and the Control of Biological Time, Harvard University Press, Cambridge, MA, 1987, Ch. 6, pp. 101–119.